PEROVSKITE SOLAR CELLS
WITH ZNS AS ELECTRON TRANSPORT LAYER

Mihail POPA[1], Anvar ZAKHIDOV[2], Ion TIGINYANU[3]

[1] Alecu Russo Balti State University, Department of Physical and Engineering Sciences,
Balti, MD-3100, Republic of Moldova
[2] University of Texas at Dallas, NanoTech Institute, Richardson, TX 75083–0688, USA.
[3] Academy of Sciences of Moldova, Institute of Electronic Engineering and Nanotechnologies "D.Chitu",
3 Academia Street 3, MD-2028, Chisinau, Republic of Moldova
Corresponding author: Mihail POPA, E-mail: `miheugpopa@yahoo.com`

Abstract. This work demonstrates the application of ZnS thin layers and the doped layers with ZnS in the perovskite solar cells. Electron transport layer has been used in three different forms. For solar cells with a single layer of ZnS – a power conversion efficiency of about 1.64 % was obtained. By using $PC_{61}BM$ fullerene layer doped with ZnS, devices with power conversion efficiency of about 3.98% were obtained, and by the application of two different layers, one of $PC_{61}BM$ and second of ZnS, solar cells with a maximum power conversion efficiency of about 5.76% were obtained.

Key words: perovskite, zinc sulfide, curent density, voltage, fill factor, efficience

1. INTRODUCTION

Use of photovoltaic cells to convert solar energy is by far the cleanest way to produce electricity. The device itself has zero emissions of greenhouse gases. At the moment, the photovoltaic cell market is dominated by those based on crystalline Si (~ 89%) and thin layers (~ 11%), mainly using CdTe and GIGS. Hybrid solar cells such as those based on sensitive pigments now represent a very small percentage of the market due to their low efficiency. Thus, efficient use of free solar energy, minimizing costs and developing large-scale applications is currently a subject of great interest. One of the main challenges of the research community is the development of materials, devices and cheaper integrated photovoltaic systems, capable of converting solar energy directly into electricity.

ZnS is a chalcogenic semiconductor compound which belongs to the family of semiconductor materials II-VI and can be crystallized in two allotropic forms: a cubic form (c-ZnS) having a sphalerite structure (or zincblende), and a hexagonal shape (h-ZnS) with wurtzite structure. The phase transition normal temperature is 1020°C, but both structures may be present at ambient temperature [1]. ZnS have a wide band gap of 3.5 – 3.8 eV at room temperature [2].

Zinc sulfide benefits from increased attention because of the wide variety of potential applications in optoelectronic devices, such as ultraviolet light-emitting diodes [3], efficient thin film phosphors for electroluminescent devices [4], buffer layer for solar cells [5–11], cathode layers for solar cells [12].

Many of the important properties of interest for such applications are determined by the microstructure of the ZnS thin film developed during the deposition process. The ZnS film's quality depends on the presence of doping elements at the growth process and post-deposition treatment [1]. ZnS thin films were prepared by various techniques, such as chemical vapor deposition (CVD) [7, 13, 14], RF magnetron sputtering [15-17], metalorganic chemical vapour deposition (MOCVD) [1], atomic layer deposition [18], pulsed-laser deposition [19], photochemical deposition [20, 21], brush plating technique [22], chemical spray pyrolysis [23], electrochemical deposition [24] and thermal evaporation [25–27]. In comparison with some sophisticated techniques, vacuum evaporation is very simple and cheap, which can be used for depositing thin films of large size. The problem associated with this technique is the maintaining stoichiometry in the deposition of materials composed from different melting points, such as ZnS.

In the last period has been manifested a strong demand for the development of buffer layers of the solar modules without Cd due to cadmium toxicity and the associated concerns about the long-term elimination of cadmium. Plane solar cells were prepared in which CdS was replaced by zinc sulfide (ZnS) as the electron transport layer. These metal sulphides have achieved success in applications as buffer layer materials to CIGS solar cells due to good optical and electrical properties. M. Nguyen et al. have reported about obtaining $ZnS/Cu_2ZnSn(SSe)_4$ (CZTSSe) solar cells, in which the ZnS buffer layer was deposited through a deposition process in the chemical bath, obtaining a power conversion efficiency of about 4.50 %, while a similar device with the CdS buffer layer has shown an efficiency of approximately 4.80 %. [11]. F.Y. Li et. al. have obtained a competitive efficiency of 11.06 % for Cd – free CIGS solar cells with ZnS buffer layer. The CIGS solar cell with CdS buffer has power conversion efficiency about 12.3% [10]. Compared with CdS buffer, the device parameters of CIGS cells with ZnS buffer are limited by their relatively low open circuit voltage (V_{oc}) and fill factor (FF). V_{oc} may be dominated by the more recombination occurring in CIGS/ZnS interface because of no buried p-n junction and big conduction band offset between CIGS and ZnS [3]. T. Nakada et al. have fabricated a chemical bath deposition – ZnS/CIGS thin film solar cell with a conversion efficiency of 18.1%, a value comparable to that of a chemical bath deposition – CdS/CIGS solar cell [2]. M.M. Islam et al. have use of ZnS/CdS double buffer layer in CIGS solar cells and was obtained higher power conversion efficiency compared to CdS/ZnS buffer layer-based CIGS cell [28]. C.J. Traverse et.al. have demonstrated efficient ZnS cathode window layers in thin-film organic photovoltaics enabled by n-type doping zinc sulfide (ZnS) with aluminum sulfide (Al_2S_3) directly through co-deposition and power conversion efficiency of devices increased from 0.6% to 1.8% [12].

Recently, organic / inorganic hybrid perovskite materials of the type ABX_3 (A = CH_3NH_3 or $HC(NH_2)_2$, B = Pb or Sn, X = I, Br or Cl) have attracted a great interest for their promising applications in solar cells as a light-gathering element and light absorption element with wide absorption spectrum and high excitonic diffusion length. Solar cells with perovskite (PSC) can reduce production costs and obtain a significantly higher energy conversion efficiency compared to standard silicon cells and other cells with thin layers [29–38]. On the other hand, zinc-based materials have recently been investigated in PSC devices as the electron transport layer for low-temperature devices, with low and flexible costs. ZnSe is a potential material for many applications due to the high mobility of electrons, high transparency and applications in various nanostructures. ZnS was introduced into the perovskite structure to improve electronic conduction [39, 40].

The purpose of this paper is to present results obtained by using thin layers of ZnS as an electron transport layer in perovskite ($CH_3NH_3PbI_3$) solar cells.

2. EXPERIMENTAL SECTION

ITO electrodes were deposited by engraving on glass. As a hole transport layer it was used PEDOT-PSS (poly (3,4-ethylenedioxythiophene) poly (styrene sulfonate)), known for ability to play the role of the holes transporter. This is deposited from 60 μl of the solution by the spin-coating method at a rotational speed of 3000 rpm for 60 s, followed by thermal treatment in air for 10 minutes at 150 ° C. The treatment time is measured using the timer on the phone.

As a bulk heterojonction it is used the lead iodide methylammonium ($CH_3NH_3PbI_3$) layer, which is a good light absorber. The perovskite layer is deposited in 80 μl of the solution through the two-stage spin-coating method: after the first deposition in 23 seconds the layer is rotated at a speed of 1000 rpm, followed by a second deposition and rotation for 30 seconds at a speed of 4000 rpm. At the 13th second after the second deposit, 150 μl of toluene is dripped. It follows heat treatment in air for 10 minutes at a temperature of 100 °C.

ZnS layer with the function of electron transport layer has been deposited by vacuum thermal evaporation at the JEOL JEE-4C vacuum evaporator. The evaporation mass was about 25 mg of ZnS powders, at the temperature of the glass substrate T_{sub} = 300 K. Vacuum pressure was about 72×10^{-4} torr, and the electric current through the evaporator was about 50 A. The Ag electrodes were deposited also by thermal evaporation in quasi-closed volume.

In another type of solar cell as electron transport layer it was used the layer deposited with 60 μl of $PC_{61}BM$ = PCBM solution (derivatized [6,6]-phenyl-C61-butyric acid methyl ester) doped with ZnS powders. The layer was deposited through the dynamic dispensing (in g-box) spin-coating in the argon chamber at a rotational speed of 1000 rpm for 40 s. It was found that the most successful solar cell was at the 1.4 mg concentration of ZnS in one ml of $PC_{61}BM$. The other layers were deposited as in the previous cells.

In the third variant of the solar cell, two layers of the electron transport layer were deposited: the first layer of ZnS was deposited by vacuum thermal evaporation under the same conditions as in the first solar cell variant; the second layer of $PC_{61}BM$ was deposited by dynamic dispensing (in g-box) spin-coating in the argon chamber at a rotation speed of 1000 rpm for 40 s. The other layers were deposited as in the previous cells.

3. RESULTS AND DISCUSIONS

The process of converting of solar energy into electrical energy takes place to the cell level in several stages. At lighting of the solar cell, the photons, whose energy is bigger than the width of the bandgap energy, are absorbed and produce excitons which are then separated from the perovskite layer into holes and electrons, after which it takes place diffusion of excitons to the regions where dissociation or separation of charges takes place and the transport of the resulting charges to the electrodes.
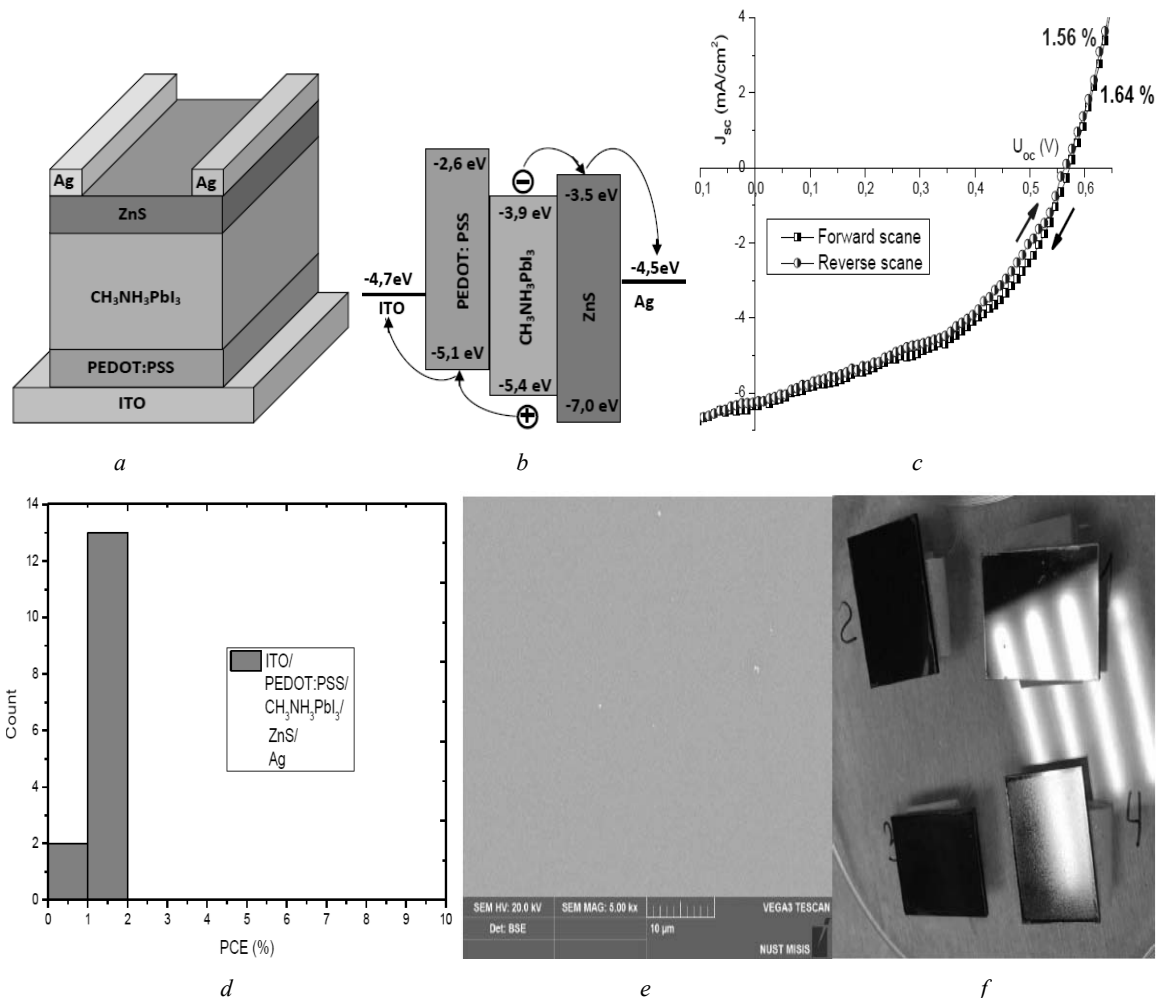
Fig. 1 – ITO/PEDOT:PSS/$CH_3NH_3PbI_3$/ZnS/Ag solar cells: device structure (*a*), the energy diagram (*b*), current density – voltage curves (*c*), histograms of PCEs (*d*), SEM image (*e*), photo solar cells (*f*).

Usually, the solar cell has a sandwich structure, where in the perovskite layer is between the electron transport layer and the holes transport layer. In Fig. 1a is presented the layered structure f the solar cell with

inverted planar architecture in which ZnS plays the role of the electron transpot layer, and the PEDOT: PSS layer – the role of hole transport layer.

In Fig. 1b is presented energy diagram of cell type ITO/PEDOT: PSS/CH$_3$NH$_3$PbI$_3$/ZnS/ Ag. It is noted that in this structure the hole passes the energy route –5.4 eV → -5.1 eV → -4.7 eV, and the electron - the energy route –3.9 eV → -3.5eV → -4.5 eV.

In Fig. 1c are presented current density – voltage characteristics of the most representative ITO/PEDOT: PSS/CH$_3$NH$_3$PbI$_3$/ZnS/Ag solar cell at forward scanning (at reducing the voltage) and reverse scanning (when increasing the voltage) and in Table 1 are presented the values of the photovoltaic parameters of the respective cells. We notice that the hysteresis of the curves is almost similar, and photovoltaic parameter values changing insignificant: the short-circuit current (J_{sc}) decreases from 6.35 mA/cm^2 to 6.27 mA/cm^2, open circuit voltage (V_{oc}) decreases from 0.57 V to 0.56 V, fill factor (FF) decreases from 44.79 % to 43.86 %, and the power conversion efficiency (PCE) evolves from 1.64 % to 1.56 %.

Table 1

Photovoltaic parameters of ITO/PEDOT:PSS/CH$_3$NH$_3$PbI$_3$/ZnS/Ag thin solar cells

Direction of scane	U_{oc} (V)	J_{sc} (mA/cm^2)	FF(%)	PCE (%)
Forward	0.57	-6.35	44.79	1.64
Reverse	0.56	-6.27	43.86	1.58

In Fig. 1d is represented a histogram of fifteen solar cells of the type ITO/PEDOT: PSS/CH$_3$NH$_3$PbI$_3$/ZnS/Ag measured under forward scanning. It is noted that thirteen devises have energy efficiency between 1-2% and only two devises have energy efficiency less than 1%.

Figure 1e shows the SEM image of the ZnS layer in the solar cell type ITO/PEDOT: PSS/CH$_3$NH$_3$PbI$_3$/ZnS/Ag. We note that the ZnS layer is uniform, without perforations, but in some places some small irregular grains appear on the surface, which probably represent some pieces of powder that have not crystallized to the surface. In Fig. 1f is presented a photograph of the samples taken until the silver electrodes are deposited. It is observed that the layers are uniform and have the same color.

a   *b*
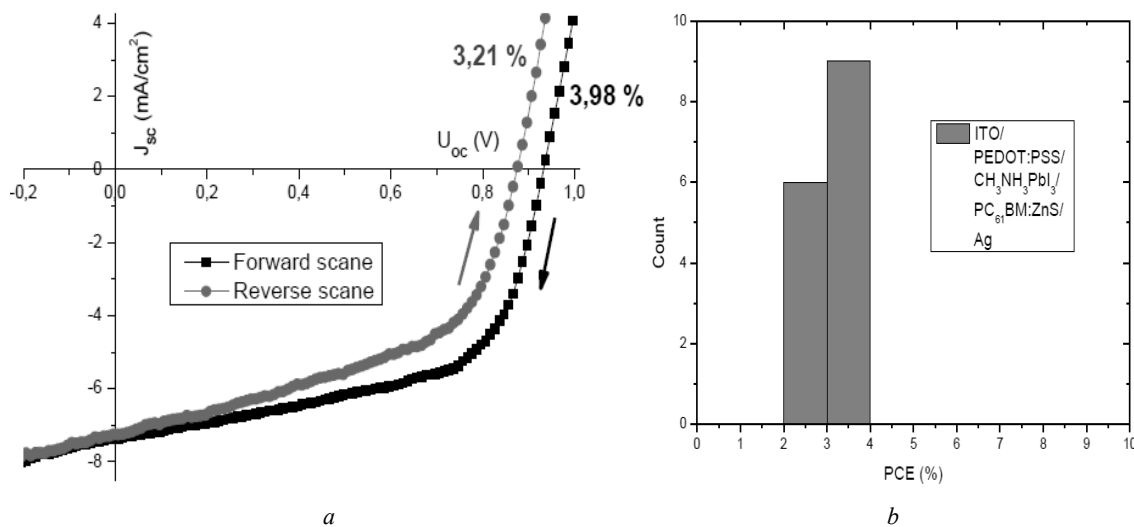
Fig. 2 – Current density – voltage characteristics of ITO/PEDOT:PSS/CH$_3$NH$_3$PbI$_3$/PC$_{61}$BM:ZnS/Ag thin solar cells (*a*), histograms of PCEs (*b*).

In another variant, as an electron transport layer the PC$_{61}$BM doped ZnS layer was used, and the other component layers of the solar cells were prepared analogously as with samples previous. In Fig. 2a shows the *J-U* curves of the most efficient solar cell type ITO/PEDOT: PSS/ CH$_3$NH$_3$PbI$_3$/PC$_{61}$BM:ZnS/Ag at forward scanning (to reduce voltage) and reverse scanning (at increased voltage), and in Table 2 are presented the values of the photovoltaic parameters of the respective cells. We note that the curve hysteresis of the reverse scanning is smaller than the forward scanning, and the photovoltaic parameter values evolves in the

following way: the short-circuit current (J_{sc}) decreases from 7.39 mA/cm^2 to 7.25 mA/cm^2, open circuit voltage (V_{oc}) decreases from 0.94 V to 0.87 V, fill factor (FF) decreases from 57.46% to 50.53%, and the power conversion efficiency (PCE) rises from 3.98% to 3.21%.

Table 2

Photovoltaic parameters of ITO/PEDOT:PSS/CH$_3$NH$_3$PbI$_3$/PC$_{61}$BM:ZnS/Ag thin solar cells

Direction of scane	U_{oc} (V)	J_{sc} (mA/cm^2)	FF(%)	PCE (%)
Forward	0.94	-7.39	57.46	3.98
Reverse	0.87	-7.25	50.53	3.21

In Fig. 2b is represented histogram of fifteen solar cells type ITO/PEDOT: PSS/CH$_3$NH$_3$PbI$_3$/ PC$_{61}$BM: ZnS/Ag measured under forward scanning. It is noted that six devises have an energy efficiency of 2–3 % and nine devises have energy efficiency ranging from 3–4%.
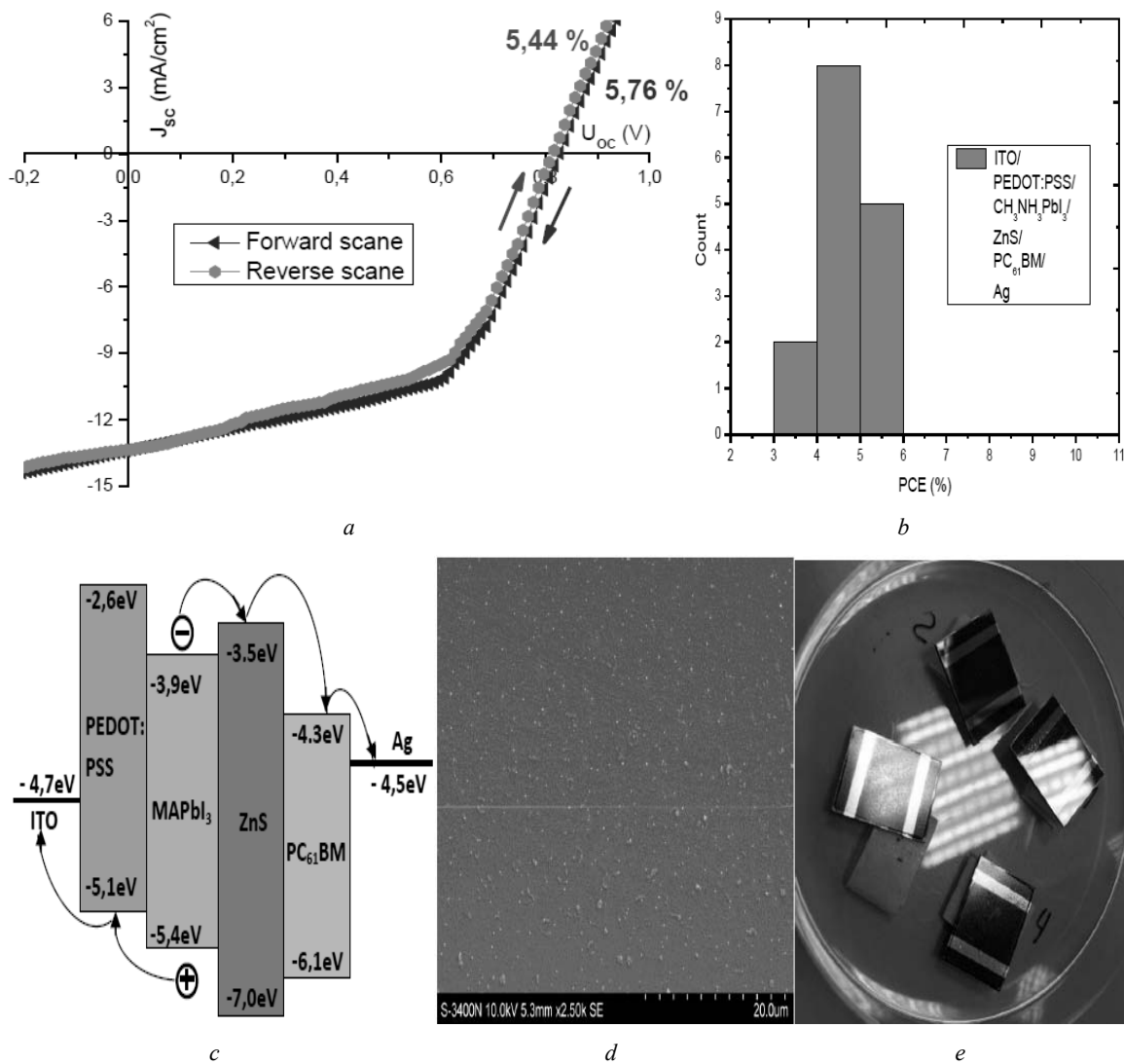
Fig. 3 – ITO/PEDOT:PSS/CH$_3$NH$_3$PbI$_3$/ZnS/PC$_{61}$BM/Ag solar cells: current density – voltage curves (*a*), histograms of PCEs (*b*), the energy diagram (*c*), SEM image of PC$_{61}$BM (*d*), photo solar cells (*e*).

The third variant of solar cells consists from two layers of electron transport layer type: one of ZnS and another by PC$_{61}$BM. In Fig. 3a are presented current density – voltage curves of the most representative solar cell type ITO/PEDOT:PSS/CH$_3$NH$_3$PbI$_3$/ZnS/PC$_{61}$BM/Ag at forward scanning (at decrease voltage) and reverse scanning (at increase voltage) and in Table 3 are presented photovoltaic values of the respective

cells. We note that curve hysteresis is almost similar, and the values of photovoltaic parameters evolve in the following way: the short-circuit current (J_{sc}) decreases from 13.51 mA/cm^2 to 13.47 mA/cm^2, open circuit voltage (V_{oc}) decreases from 0.82 V to 0.81 V, fill factor (FF) decreases from 52.17 % to 50.58 %, and the power conversion efficiency (PCE) is changing from 5.76 % to 5.44 %.

Table 3

Photovoltaic parameters of ITO/PEDOT:PSS/CH$_3$NH$_3$PbI$_3$/ZnS/PC$_{61}$BM/Ag thin solar cells

Direction of scane	U_{oc} (V)	J_{sc} (mA/cm^2)	FF(%)	PCE (%)
Forward	0.82	-13.51	52.17	5.76
Reverse	0.81	-13.47	50.58	5.44

In Fig. 3b is represented a histogram of fifteen solar cells of type ITO / PEDOT: PSS / CH$_3$NH$_3$PbI$_3$/ZnS/PC$_{61}$BM/Ag measured under forward voltage scanning. It is noted that two devises have an energy efficiency between 3–4%, eight devices have an energy efficiency of 4-5%, and five devises have an energy efficiency between 5–6%.

In Fig. 3c is presented energy diagram of solar cells type ITO/PEDOT: PSS/CH$_3$NH$_3$PbI$_3$/ZnS/ PC$_{61}$BM/Ag. We note that this structure simplifies the electron route from perovskite to Ag electrode by making smaller cascade jump between closer energy levels (from 3.9 eV to 3.5 eV, then to 4.3 eV to 4.5 eV). This probably also explains the increase in PCE of these cells relative to other devices.

In Fig. 3d is presented the SEM image of an cell type ITO/PEDOT: PSS / CH$_3$NH$_3$PbI$_3$/ZnS/PC$_{61}$BM/Ag. It is noted that the surface is uniform with small formations of different shapes. In Fig. 3e there is a photograph of the samples taken after the deposition of the silver electrodes. It is observed that the layers are uniform and have the same color.

In the paper [39] an analogous cascade structure has been described in which the electron transport layer of the solar cell consists of two thin layers: one of ZnS and another of TiO$_2$, resulting in an efficient conversion of 4.90 % at forward scanning and 5.27 % at reverse scanning. Jiang Liu [40] were prepared solar cell types ITO/ZnS/perovskite/spiro-OMeTAD/Au, obtaining a power conversion efficienty of 0.98 %.

4. CONCLUSION

In this work we have demonstrated the use in different structures of zinc sulphide as an electron transfer layer in perovskite solar cells with inverse planar architecture. The advantages of these cells would be their preparation at low temperatures by two relatively cheap methods: spin-coating and thermal evaporation. Moving the conduction band to the interface between perovskite and electron transport layer have proven to be very successful in reducing energy losses for transporting and collecting charges and reducing the load carrier recombination. I believe that the successful use of ZnS thin films (and ZnS-doped solutions) in perovskite-based solar cells can extend to several inorganic semiconductor materials, including n-type semiconductors (CdSe, ZnSe, In2S3 etc).

From the point of view of toxicity, ZnS is, undoubtedly, a better candidate than CdS or CdSe, which makes it more suitable for incorporation into such solar cells.

REFERENCES

1. T. KRYSHTAB, V.S. KHOMCHENKO, J.A. ANDRACA-ADAME, V.E. RODIONOV, V.B. KHACHATRYAN, YU.A. TZYRKUNOV, *The influence of doping element on structural and luminescent characteristics of ZnS thin films*, Superlattices and Microstructures, **40**, pp. 651–656, 2006.
2. R. JOHN, S.S. FLORENCE, *Optical, structural and morphological studies of bean-like ZnS nanostructures by aqueous chemical method*, Chalcogenide Letters, **7**, *4*, pp. 269 – 273, 2010.
3. J. KWAK, J. LIM, M. PARK, S. LEE, K. CHAR, CH. LEE, *High-Power Genuine Ultraviolet Light-Emitting Diodes Based On Colloidal Nanocrystal Quantum Dots*, Nano Letters, doi: 10.1021/acs.nanolett.5b0039.
4. V. DIMITROVA, J. TATE, *Synthesis and characterization of some ZnS-based thin film phosphors for electroluminescent device applications*, Thin Solid Films, **365**, pp.134-138, 2000.
5. T. NAKADA, M. MIZUTANI, *18% Efficiency Cd-Free Cu(In, Ga)Se2Thin-Film Solar Cells Fabricated Using Chemical Bath Deposition (CBD)-ZnS Buffer Layers*, Japan J. Appl. Phys., **41**, pp. 165–167, 2002.

6. T. NAKADA, M. HONGO , E. HAYASHI, *Band offset of high efficiency CBD-ZnS / CIGS thin film solar cells*, Thin Solid Films, **431–432**, pp. 242–248, 2003.

7. A. GOUDARZI, G. M. AVAL, R. SAHRAEI, H. AHMADPOOR, *Ammonia-free chemical bath deposition of nanocrystallineZnS thin film buffer layer for solar cells*, Thin Solid Films, **516**, pp. 4953–4957, 2008.

8. L.LARINA, D. SHIN, J.H. KIM, B. T. AHN, *Alignment of energy levels at the ZnS/Cu(In,Ga)Se2interface*, Energy Environ. Sci., **4**, pp. 3487, 2011.

9. N. NAGHAVI, T. HILDEBRANDT, G. RENOU, S. TEMGOUA, JF. GUILLEMOLES, D. LINCOT, *Impact of the deposition conditions of window layers on lowering the metastability effects in Cu(In,Ga)Se2/CBD ZnS-based solar cell*, Mater. Res. Soc. Symp. Proc., **1538**, 2013, Materials Research Society, DOI: 10.1557/opl.2013.

10. F.Y. LI, X.Y DANG, L.ZHANG, F.F LIU, D.SUN, Q.HE, C.J. LI, B.Z. LI, H.B. ZHU, *Fabrication of high-quality ZnS buffer and its application in Cd-free CIGS solar cells*, Optoelectronics Letters, **10**, *4*, 2014

11. M. NGUYEN,K. ERNITS, K. F. TAI, C. F. NG, S.S. PRAMANA, W.A.SASANGKA, S.K. BATABYAL, T. HOLOPAINEN, D. MEISSNER, A. NEISSER, L.H.WONG, *ZnS buffer layer for Cu2ZnSn(SSe)4monograin layer solar cell*, Solar Energy, **111**, pp. 344–349, 2015

12. C.J. TRAVERSE, M. YOUNG, S. WAGNER, P.ZHANG, P. ASKELAND, M.C. BARR, R.R. LUNT, *Efficient zinc sulfide cathode layers for organic photovoltaic applications via n-type doping*, Journal of Applied Physics, **115**, pp. 194505, 2014.

13. Q. LIU, M. GUOBING, A. JIANPING, *Chemical bath-deposited ZnS thin films: Preparation and characterization*, Applied Surface Science, **254**, pp. 5711–5714, 2008.

14. A. WEI, J. LIU, M. ZHUANG, Y. ZHAO, *Preparation and characterization of ZnS thin films prepared by chemical bath deposition*, Materials Science in Semiconductor Processing, **16**, pp. 1478–1484, 2013.

15. M.A. TAGLIENTE, M. PENZA, M. GUSSO, A. QUIRINI, *Characterisation of ZnS:Mn thin films by Rietveld refinement of Bragg-Brentano X-ray diffraction patterns*, Thin Solid Films, **353**, pp. 129-136, 1999.

16. P.K. GHOSH, S. JANA, S. NANDY, K.K. CHATTOPADHYAY, *Size-dependent optical and dielectric properties of nanocrystalline ZnS thin films synthesized via rf-magnetron sputtering technique*, Materials Research Bulletin, **42**, pp. 505–514, 2007.

17. D.H. HWANG, J. H. AHN, K. N. HUI, K. S. HUI, Y.G. SON, *Structural and optical properties of ZnS thin films deposited by RF magnetron sputtering,* Nanoscale Research Letters, **7**, *26*, 2012.

18. Y.S. KIM, S. J. YUN*, Studies on polycrystalline ZnS thin films grown by atomic layer deposition for electroluminescent applications,* Applied Surface Science, **229**, pp.105–111, 2004.

19. S. YANO, R. SCHROEDER ,B. ULLRICH , H. SAKAI, *Absorption and photocurrent properties of thin ZnS films formed by pulsed-laser deposition on quartz*, Thin Solid Films, **423**, pp. 273–276, 2003.

20. M. GUNASEKARAN, R. GOPALAKRISHNAN, P. RAMASAMY, *Deposition of ZnS thin films by photochemical deposition technique,* Materials Letters, **58**, pp. 67–70, 2003.

21. T. MIYAWAKI, M. ICHIMURA, *Fabrication of ZnS thin films by an improved photochemical deposition method and application to ZnS/SnSheterojunction cells*, Materials Letters, **61**, pp. 4683–4686, 2007.

22. K.R. MURALI, S. VASANTHA, K. RAJAMMA, *Properties of pulse plated ZnS films*, ECS Transactions, **11**, *28*, pp. 91-96, 2008.

23. P. O. OFFOR, B.A. OKORIE, B. A. EZEKOYE, V. A. EZEKOYE, J. I. EZEMA, *Chemical spray pyrolysis synthesis of zinc sulphide (ZnS) thin films via double source precursors*, Journal of Ovonic Research, **11**, *2*, pp.73 – 77, 2015.

24. O.K. ECHENDU, A.R. WEERASINGHE, D.G. DISO, F. FAUZI, I.M. DHARMADASA, *Characterization ofn-Type andp-Type ZnS Thin Layers Grown by an Electrochemical Method*, Journal of Electronic Materials, **42**, *4*, 2013.

25. H. R. DIZAJI, A.J. ZAVARAKI, M. H. EHSANI, *Effect of thickness on the structural andoptical properties of ZnS thin films prepared by flash evaporation technique equippedwith modified feeder*, Chalcogenide Letters, **8**, *4*, pp. 231 – 237, 2011.

26. X. WU, F. LAI, L. LIN, J. LV, B. ZHUANG, Q. YAN, Z. HUANG, *Optical inhomogeneity of ZnS films deposited by thermal evaporation*, Applied Surface Science, **254**, pp. 6455–6460, 2008.

27. T.G. KRYSHTAB, V.S. KHOMCHENKO, V.P. PAPUSHA , M.O. MAZIN, YU.A. TZYRKUNOV, *Thin ZnS:Cu,Ga and ZnO:Cu,Ga film phosphors*, Thin Solid Films, **403–404**, pp. 76–80, 2002.

28. M.M. ISLAM, S. ISHIZUKA, A. YAMADA, K. SAKURAI, S. NIKI, T. SAKURAI, K. AKIMOTO, *CIGS solar cell with MBE-grown ZnS buffer layer*, Solar Energy Materials & Solar Cells, **93**, pp. 970–972, 2009.

29. J.H. IM, CH.R. LEE, J.W. LEE, S.W. PARK, N.G. PARK, *6.5% efficient perovskite quantum-dot-sensitized solar cell*, Nanoscale, **3**, pp. 4088, 2011.

30. W. QARONY , Y. A. JUI, G. M. DAS, T. MOHSIN, M. I. HOSSAIN, S. N. ISLAM, *Optical Analysis in CH3NH3PbI3 and CH3NH3PbI2Cl Based Thin-Film Perovskite Solar Cell*, American Journal of Energy Research, **3**, *2*, pp. 19-24, 2015.

31. J.S. SHAIKH, N.S. SHAIKH, A. D.SHEIKH, S.S.MALI, A.J.KALE, P. KANJANABOOS, C. K. HONG, J.H.KIM, P.S.PATIL, *Perovskite solar cells: In pursuit of efficiency and stability*, Materials & Design, **136**, pp. 54-80, 2017.

32. I. MESQUITA, L. ANDRADE, A. MENDES, *Perovskite solar cells: Materials, configurations and stability*, Renewable and Sustainable Energy Reviews, **82**, *3*, pp. 2471-2489, 2018.

33. S.D. STRANKS, G.E. EPERON, G.GRANCINI, C.MENELAOU, M. J. P. ALCOCER,T. LEIJTENS, L.M. HERZ, A. PETROZZA, H. J. SNAITH, *Electron-Hole Diffusion Lengths Exceeding 1 Micrometer in an OrganometalTrihalidePerovskite Absorber*, Science, **341**, pp. 342, 2013.

34. H. ZHOU, Q. CHEN, G. LI, S. LUO, T. SONG, H.-S. DUAN, Z. HONG, J. YOU, Y. LIU, Y. YANG, *Interface engineering of highly efficient perovskite solar cells*, Science*, 345*, 6196, pp. 542-546, 2014.

35. C. O. R. QUIROZ, I. LEVCHUK, C. BRONNBAUER, M. SALVADOR, K. FORBERICH, T. HEUMULLER, Y. HOU, P. SCHWEIZER, E. SPIECKERD AND C. J. BRABECAE, *Pushing efficiency limits for semitransparent perovskite solar cells*, J. Mater. Chem. A, **3**, pp. 24071–24081, 2015.

36. J.-P. CORREA-BAENA, A. ABATE, M. SALIBA, W. TRESS, T. J. JACOBSSON, M. GRATZEL, A. HAGFELDTA, *The rapid evolution of highly efficient perovskite solar cells*, Energy Environ. Sci., **10**, pp. 710—727, 2017.

37. S. DE WOLF, J. HOLOVSKY, S.-J. MOON, P. LÖPER, B. NIESEN, M. LEDINSKY, F.-J. HAUG, J.-H. YUM, C. BALLIF, *Organometallic Halide Perovskites: Sharp Optical Absorption Edge and Its Relation to Photovoltaic Performance*, J. Phys. Chem. Lett., **5**, *6*, pp. 1035–1039, 2014.

38. V.A. MILICHKO, A.S. SHALIN, I.S. MUKHIN, A.E. KOVROV, A.A. KRASILIN, A.V. VINOGRADOV, P.A. BELOV, C.R. SIMOVSKII, *Solar photovoltaics, Current state and trends*, **59**, pp. 727–772, 2016.

39. W.KE, C.C.STOUMPOS, J.L. LOGSDON, M.R. WASIELEWSKI, Y. YAN, G. FANG, M.G.KANATZIDIS, *TiO_2-ZnS Cascade Electron Transport Layer for Efficient Formamidinium Tin Iodide Perovskite Solar Cells*, J. Am. Chem. Soc., **138**, pp. 14998−15003, 2016.

40. J. LIU, C. GAO, L. LUO, Q. YE, X. HE, L. OUYANG,X. GUO, D. ZHUANG, C. LIAO, J. MEI, W. LAU, *Low-temperature, solution processed metal sulfide as an electron transport layer for efficient planar perovskite solar cells*, Journal of Materials Chemistry A, **3**, pp. 11750-11755, 2015.